

Structural identification and seismic performance of brick chimneys, Tokoname, Japan

T. Aoki†

*Graduate School of Design and Architecture, Nagoya City University,
Kitachikusa 2-1-10, Chikusa-ku, 464-0083 Nagoya, Japan*

D. Sabia‡

*Department of Structural and Geotechnical Engineering, Politecnico di Torino,
Corso Duca degli Abruzzi 24, 10129 Turin, Italy*

(Received March 4, 2005, Accepted September 1, 2005)

Abstract. Dynamic and static analyses of existing structures are very important to obtain reliable information relating to actual structural properties. For this purpose a series of material test, dynamic test and static collapse test of the existing two brick chimneys, in Tokoname, are carried out. From the material tests, Young's modulus and compressive strength of the brick used for these chimneys are estimated to be 3200 MPa and 7.5 MPa, respectively. The results of static collapse test of the existing two brick chimneys are discussed in this paper and composed with the results from FEA (Finite Element analysis). From the results of dynamic tests, the fundamental frequencies of Howa and Iwata brick chimneys are estimated to be about 2.69 Hz and 2.93 Hz, respectively. Their natural modes are identified by ARMAV (Autoregressive Moving Average Vectors) model. On the basis of the static and dynamic experimental tests, a numerical model has been prepared. According to the European code (Eurocode n. 8: "Design of structures for earthquake resistance") non-linear static (Pushover) analysis of the two chimneys is carried out and they seem to be vulnerable to earthquakes with 0.25 to 0.35 g.

Key words: brick chimney; dynamic test; static collapse test; identification; ARMAV; non-linear analysis; pushover analysis.

1. Introduction

Tokoname City, Aichi Prefecture, is located in the center of the west coast of the Chita Peninsula, facing Ise Bay to the west and hilly terrain extends to the east. Tokoname has long been noted for its production of ceramic ware, and its history dates back to nearly 1,000 years ago. Along with Seto, Shigaraki, Echizen, Tanba, and Bizen, Tokoname is included in the Rokkoyo (the nation's six oldest ceramic producing districts). And Tokoname is said to be the oldest and largest kiln site of them all. Even today, Ceramics is one of the major industries in Tokoname where the tradition and culture of Tokoname ware are still alive. The Central Japan International Airport on the offshore

† Associate Professor, Corresponding author, E-mail: aoki@sda.nagoya-cu.ac.jp

‡ Associate Professor



Photo 1 Landscape of Tokoname city (offered by K. Sughie)

waters of Tokoname City was opened on 17 February 2005 (Tokoname City web site).

Pottery has been a dramatically growing industry since the Meiji period when ceramic pipes started to be used for drainage. These days, industrial materials or products such as sanitary wares and ceramic tiles are eagerly produced. “Tokoname ware” includes a wide range of products from tea-implements, flower vases, bonsai pots, and ceramic ornaments to a new series of products such as “handmade tableware” which meet the demands of the present age while preserving the tradition (Tokoname City web site).

Until the first half of the Showa period, there were over 300 chimneys in Tokoname. Some were destroyed by typhoons and/or earthquakes. Unfortunately, due to their vulnerability to typhoons and/or earthquakes, chimneys which were not used were pulled down, or reduced to half height, so that now, the number of chimneys has decreased to 119 (Photo 1).

Based on results of an investigation into the history of earthquakes, an interval of about 100 to 150 years can be expected in the Tokai - Nankai area, and there is rising concern that an earthquake of magnitude 8 class will occur in the first half of this century. The purpose of this paper is to obtain data concerning the static and dynamic structural properties of brick chimneys in Tokoname in order to preserve them (Aoki *et al.* 2004).

2. Chimneys in Tokoname

An investigation of chimneys executed by T. Kakita in August 1995 revealed that there were 152 chimneys including 55 perfect brick ones. Unfortunately, the number of Chimneys has decreased to 119 including 45 perfect brick ones in January 2003 (Aoki 2004). Howa and Iwata brick chimneys were destroyed due to construction of an access road to the Central Japan International Airport in January 2003 (Photo 2 and Fig. 1). However, fortunately an opportunity to investigate these two brick chimneys was available.

Profiles of the Howa and Iwata brick chimneys are listed in Table 1. Fig. 2 shows the proportions of the existing chimneys in Tokoname. As shown in Fig. 2, the proportions of these two brick chimneys are standard in Tokoname.

Electromagnetic Radar was applied in order to estimate their thickness. The thickness of the Howa brick chimney changes four times from the top to the bottom, that is, 0.21 m, 0.315 m,



Photo 2 Brick chimneys

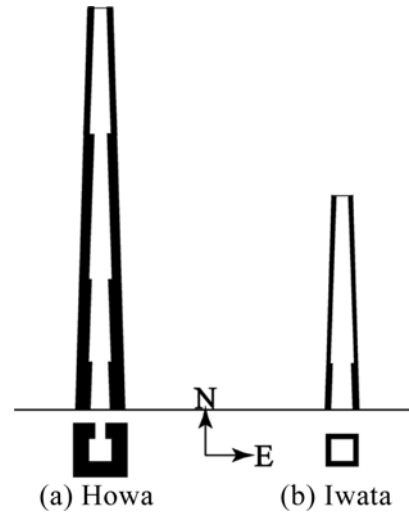


Fig. 1 Plan and section

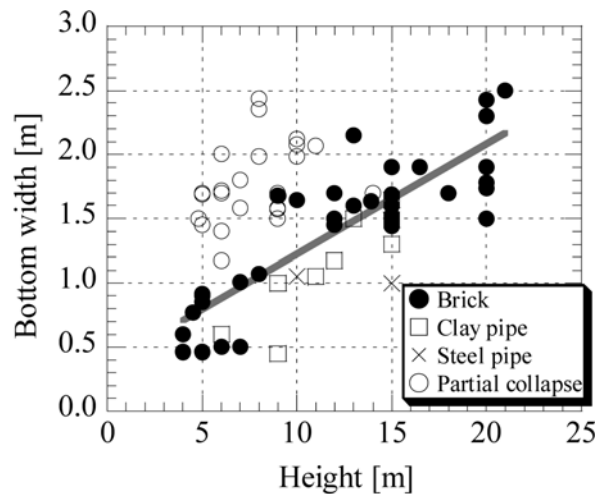


Fig. 2 Proportions of chimneys in Tokoname

Table 1 Profiles of Howa and Iwata brick chimneys (m)

	Height	Bottom width	Top width	Bottom thickness	Top thickness
Howa	15.0	1.96	1.06	0.53	0.21
Iwata	8.2	1.16	0.68	0.21	0.11

0.42 m, and 0.53 m. On the other hand, the thickness of the Iwata brick chimney changes from 0.11 m at the top to 0.21 m at the bottom (Fig. 1). As for the Howa brick chimney, four iron angles of 75 mm × 75 mm × 6 mm at corners are fastened by 12 series of iron ties of ϕ 16 mm. On the other hand, four iron angles of 40 mm × 40 mm × 3 mm at corners are fastened by 6 series of iron ties of ϕ 9 mm in the Iwata brick chimney.

3. Material tests

In order to estimate Young's modulus and compressive strength of the brick used for these brick chimneys, core sampling tests are carried out. The diameter and the height of the brick specimens are about 33 mm and 50 mm, respectively. From the material tests, Young's modulus and compressive strength of the brick are estimated to be 3200 MPa and 7.5 MPa, respectively (Aoki 2004). The specific gravity of the brick is determined about 16.5 kN/m³.

4. Static collapse test

For the purpose of obtaining the data concerning static structural properties of brick chimneys in Tokoname to preserve them, pull down tests of Howa and Iwata brick chimneys are carried out (Photos 3 and 4).



(a) Crack at the middle height



(b) Collapse

Photo 3 Static collapse test of Howa brick chimney



(a) Crack at the base



(b) Collapse

Photo 4 Static collapse test of Iwata brick chimney

To the upper part of the brick chimneys, wire rope was set up and it was pulled by a derrick car until their collapse. During the static collapse test, horizontal load and deformation at the top of the brick chimneys are measured by means of load cell and laser range finder, respectively.

Ultimate horizontal loads of Howa and Iwata brick chimneys are 32.15 kN (horizontal component is 29.13 kN) and 4.40 kN (horizontal component is 4.25 kN), respectively. Collapse modes are different between Howa and Iwata brick chimneys. In case of Howa brick chimney, collapse occurs at the middle height of the chimney, that is, 8 m height from ground level which is shown in Photo 3. On the other hand, as shown in Photo 4, collapse of Iwata brick chimney occurs at the base of the chimney.

Fig. 3 shows relationship between height and bending moment in Howa brick chimney. In Fig. 3, solid line shows the admissible bending moment determined by static equilibrium and dotted line represents the bending moment produced by the same loading condition of static collapse test (Static). From this Figure, it is to note that collapse of Howa brick chimney occurs at the middle height of the chimney, that is 8 m height from ground level. From static equilibrium, tensile strength of the brick chimney is estimated to be 0.37 MPa. Dashed line and chain double-dashed line represent the bending moments under the condition of lateral loads proportional to mass (Case 1) and to 1st mode shape (Case 2), respectively (see section 8.1, 1), a) and b)).

5. Dynamic test

5.1 Microtremor measurement

For the purpose of obtaining the data concerning dynamic structural properties of Howa brick chimney, as a first phase of dynamic test, microtremor by ambient vibrations are measured at the top. Smoothed spectra by Parzen's spectral window of 0.5 Hz are given in Fig. 4. In Fig. 4, bold solid line, bold dotted line and fine solid line show the spectra in north-south, east-west and vertical

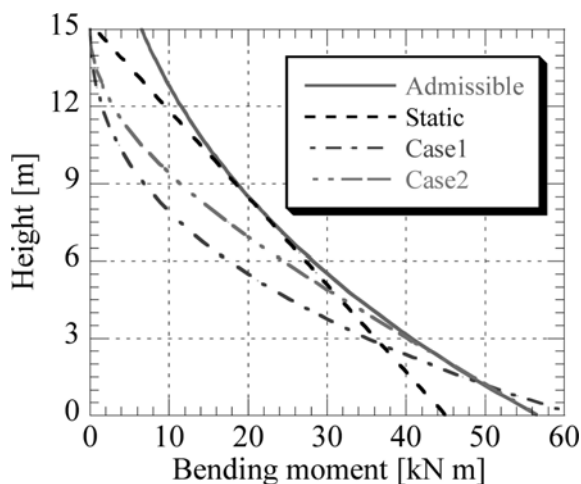


Fig. 3 Relationship between height and bending moment (Howa brick chimney)

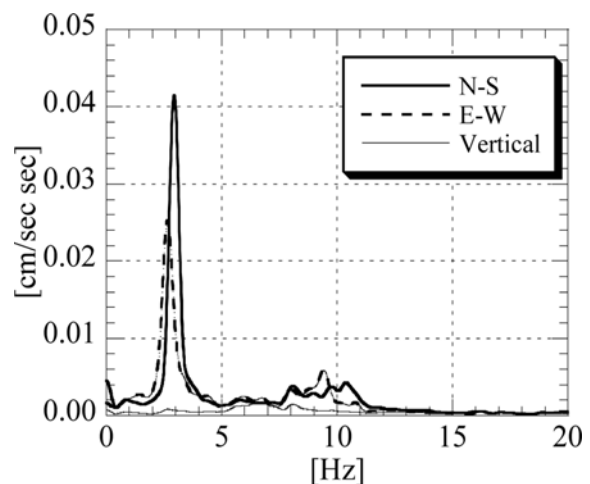


Fig. 4 Spectra observed in microtremors (Howa brick chimney)

directions, respectively. According to the observation of microtremor measurement, the fundamental frequencies of Howa brick chimney are estimated to be 2.95 Hz and 2.67 Hz in north-south and east-west directions, respectively. There is difference between two directions due to the window in north side (Fig. 1).

5.2 Acceleration measurement

In the second phase of dynamic test, as for both Howa and Iwata brick chimneys, acceleration of 6 points is contemporaneously measured in north-south or east-west directions. One sensor is placed at the base of the chimney and another one is placed at the top. Other sensors are equally spaced along the chimney. Excitation is ground motion due to derrick car.

6. Dynamic identification

The experimental dynamic parameters such as fundamental frequencies and mode shapes are identified by analysis of the accelerations time-history by means of ARMAV (Autoregressive Moving Average Vectors) techniques.

6.1 The ARMAV technique

An ARMAV model (Marple 1987, Olafsson *et al.* 1995, De Stefano *et al.* 1997, 2001, Andersen *et al.* 1996, 1998, Giorcelli *et al.* 1998, Garibaldi *et al.* 1999, 2001, Peeters *et al.* 2001, Sabia *et al.* 2003) can be expressed in the state space according to the following expression (u and x are the input and output):

$$\{\bar{x}[n]\} = [a]\{\bar{x}[n-1]\} + [b]\{\bar{u}[n]\} \quad (1)$$

In these parametric models the system output $\bar{x}[n]$ is supposed to be caused by a white noise input $\bar{u}[n]$ and the algorithm estimates the parameters' values that minimize the residual variance. The parameter estimation algorithm works as follows: a first ARV model, whose structure is

$$\bar{x}[n] = \sum_{k=1}^p \hat{A}[k]\bar{x}[n-k] + \hat{u}[n] \quad (2)$$

is fitted to the data. Using the estimated autoregressive parameters $\hat{A}[k]$, the residual vector $\hat{u}[n]$ is computed and used as input for the ARMAV model:

$$\bar{x}[n] = \sum_{k=1}^p \hat{A}[k]\bar{x}[n-k] + \hat{u}[n] + \sum_{k=1}^q \hat{B}[k]\hat{u}[n-k] \quad (3)$$

An iterative procedure can then be started, to alternately refine the estimated parameters $\hat{A}[k]$, $\hat{B}[k]$ and the residual $\hat{u}[n]$ to minimize the residual variance. The procedure ends when the difference between the parameters $\hat{A}[k]$ and $\hat{B}[k]$, estimated in two consecutive iterations, is smaller than a desired value.

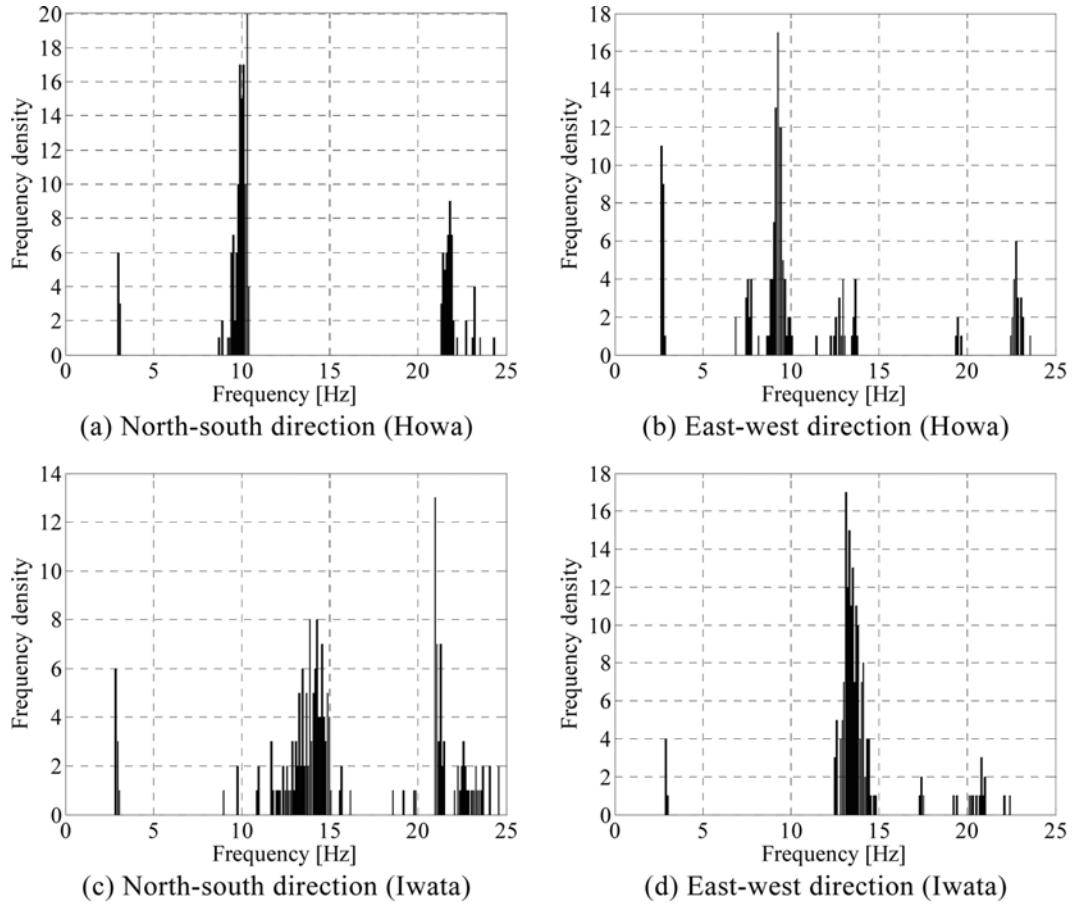


Fig. 5 Frequency distributions identified by ARMAV model

Table 2 Fundamental frequencies identified by ARMAV model

		Direction	Mode	Frequency (Hz)
Howa	North-South		1st	3.0603
			2nd	9.9725
			3rd	22.3372
	East-West		1st	2.6918
			2nd	9.3494
			3rd	22.7584
Iwata	North-South		1st	2.9330
			2nd	14.4932
			3rd	21.8729
	East-West		1st	2.9356
			2nd	13.7789
			3rd	19.9204

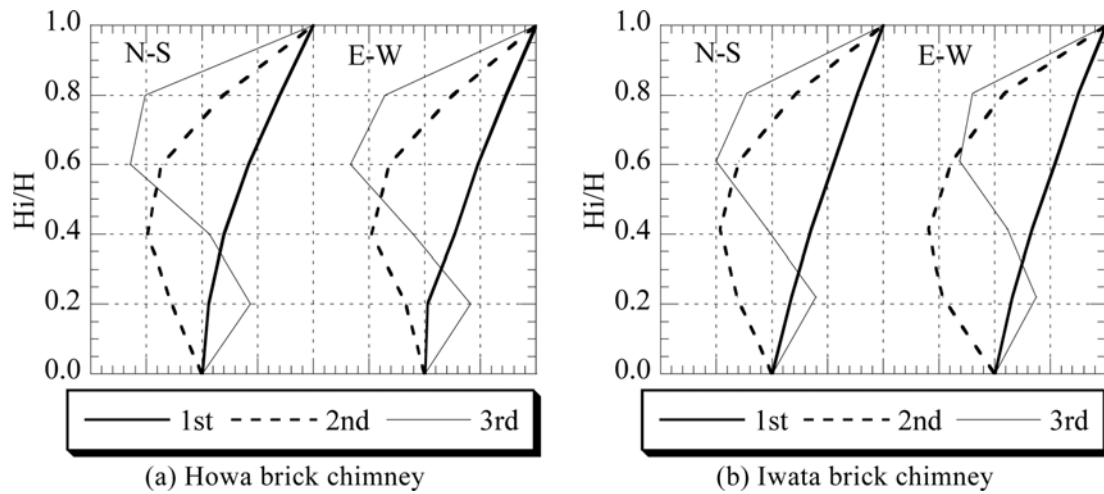


Fig. 6 Natural mode shapes identified by ARMAV model

6.2 Results of dynamic identification

In Fig. 5, the frequency distributions of Howa and Iwata brick chimneys identified by the ARMAV model considering the complete time record are depicted in north-south and east-west directions, respectively. Fundamental frequencies identified by the ARMAV model are listed in Table 2.

Fig. 6 shows natural mode shapes in both two orthogonal directions identified by the ARMAV model. As for the mode shapes, especially first mode shape, there is difference between Howa and Iwata brick chimneys due to boundary condition. The foundation of Howa brick chimney is made in reinforced concrete, and on the other hand, that of Iwata brick chimney is made in sand (Photo 4(b)).

7. Static non-linear analysis

7.1 Numerical model

The FEM (Finite Element Method) has become one of the most important and useful engineering tools for civil engineers. In order to analyze masonry structures, mathematical models are developed to describe their behaviors. While developing the mathematical models, some assumptions are made for simplification. Definitely masonry material can resist high compressive stresses but only feeble tensions. Conventional assumptions on masonry are made such that no sliding failure, no tensile strength and infinite compressive strength, and some rigid behavior due to compression.

There are mainly two approaches for the analysis of masonry structures by means of FEM, one is macro-modeling and the other is micro-modeling. The most widely used macro-modeling is based on the assumption of isotropy and homogeneity for material, Drucker-Prager plastic failure criterion with low-level cut-off on tensile stresses (Anthoine 1995). Other FEA non-linear models are based on the damage mechanics. Cracks are assumed to form in planes perpendicular to the direction of

maximum principal tensile stress which reaches the specified tensile strength. Anisotropic continuum model (Lourenço *et al.* 1995, Aoki *et al.* 2001) and continuum model (Gamberotta *et al.* 1997b) are applied for masonry walls. For sufficiently large structures, the global response of masonry can be well predicted even without the inclusion of the local interaction between the masonry components.

For the micro-modeling of masonry, composite interface model (Lourenço *et al.* 1995), mortar joint model (Gamberotta *et al.* 1997a), elastic-plastic joint element (Kato *et al.* 1986, Aoki 2001), and Bott-Duffin inverse (Aoki *et al.* 2003a, 2003b) are applied for the non-linear behavior of masonry confining the elastic-plastic failure to mortar bed-joints. As has been shown by the analysis of discontinuous rocks, the joint element is effectively modeled for analyzing structures composed of two different materials with very different strength such as masonry arches. The micro-modeling is capable for describing the local interaction between masonry components, however, it becomes very difficult to solve for sizable masonry structures in which interfaces increase.

For the above reason, on the basis of the static and dynamic experimental tests, numerical model has been prepared. As shown in Figs. 9 and 10, analytical model is composed of 9-node isoparametric Heterosis shell elements which is consisted of eight layers. The FEM based on isoparametric degenerated shell elements is adopted for the numerical analysis (Ahmad *et al.* 1970, Zienkiewicz 1971, Hughes *et al.* 1978, 1986, Hinton *et al.* 1984, Aoki *et al.* 1997). The selective integration rule is adopted for numerical integration. Total numbers of nodes and elements are 1476 and 320, respectively (Figs. 9 and 10).

Masonry is an anisotropic material. Therefore, the biaxial strength envelope of masonry must be either described in terms of the full stress vector in a fixed set of material axes, or in terms of principal stresses and the rotation angle between the principal stresses and the material axes (Page 1981, 1983). The tests have been carried out with half scale solid clay units. Both the orientation of the principal stresses with regard to the material axes and the principal stress ratio considerably

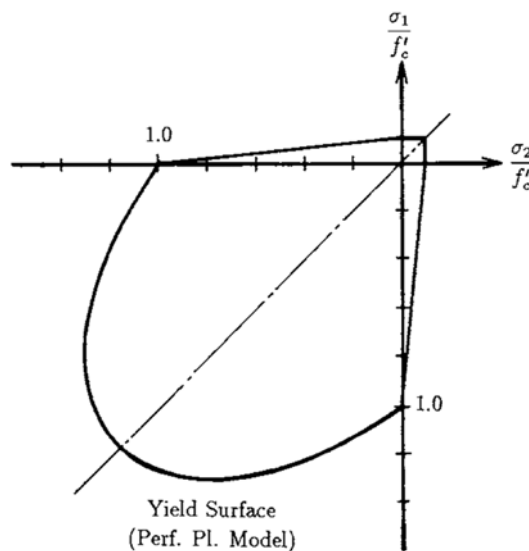


Fig. 7 Yielding condition for concrete constitutive model

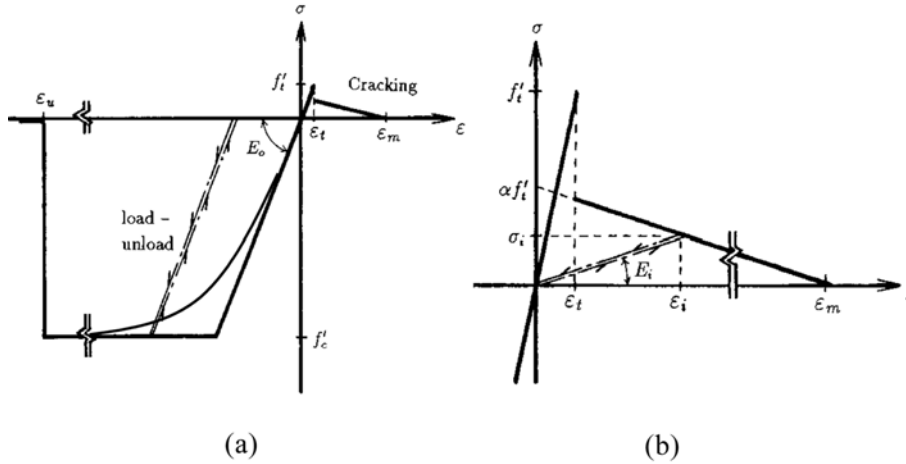


Fig. 8 Stress-strain relationship for concrete constitutive model

influence the failure mode and strength. From the experimental results by Page (1981, 1983), Magenes *et al.* (1995, 1997), however, the following yielding surface, given by Eq. (4), for the FEM analysis is applied in this paper (Fig. 7). The yielding condition of bi-axial compressive masonry is expressed on the basis of the Duruker-Prager yielding condition. The yielding function depends on the mean normal stress I_1 and the second stress invariant J_2 as follows,

$$f(I_1, J_2) = [\beta(3J_2) + \alpha I_1]^{1/2} = \bar{\sigma} \quad (4)$$

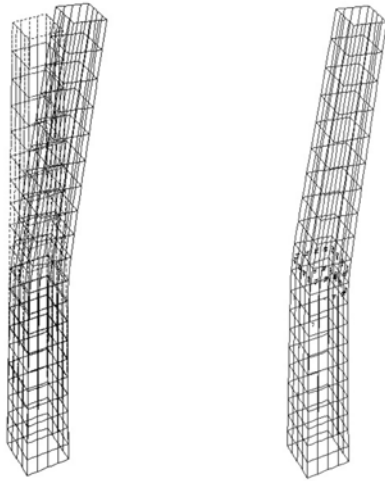
where $\alpha = 0.355\bar{\sigma}$ and $\beta = 1.355$ are adopted, based on the experimental data by Page and Magenes also taken into consideration the results by Kupfer *et al.* (1969, 1973).

The masonry is assumed to yield in compression when the equivalent stress $\bar{\sigma}$ reaches to 30% of uni-axial compressive strength, and the flow rule proposed by Prandtl-Reuss is applied to the masonry in the plastic phase. The hardening rule of masonry is assumed based on the equivalent uni-axial stress-strain relation defined by the conventional Madrid parabola.

Fig. 8 shows the stress-strain relationship of concrete characterizing the element. The crush of masonry is judged by equivalent strain. The function is defined by replacing the stress components of the yield function with the strain components. The masonry is assumed to crush when the equivalent strain ε reaches the ultimate strain ε_u , and the analysis is performed under a condition that the stiffness after this strain has to be zero (Fig. 8(a)).

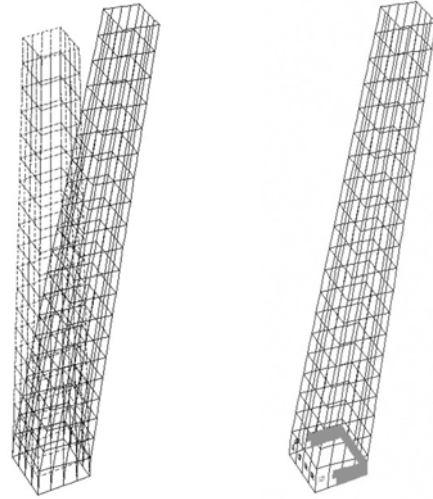
The crack of masonry is assumed to occur when the tensile principal stress exceeds the tensile ultimate strength shown in Fig. 8(b). Cracks are assumed to form in planes perpendicular to the direction of maximum principal tensile stress which reaches the specified tensile strength. The cracked masonry is anisotropic and smeared crack model is adopted. After cracking, for the sake of the expediency to achieve numerical efficiency, a small amount of tension stiffening is assumed in uni-axial stress-strain relationships represented as follows,

$$\sigma_i = \alpha \cdot f'_t \cdot (1 - \varepsilon_i / \varepsilon_m), \quad \varepsilon_t \leq \varepsilon_i \leq \varepsilon_m \quad (i = 1, 2) \quad (5)$$



(a) Deformation (b) Crack pattern

Fig. 9 Result of FEA of Howa brick chimney



(a) Deformation (b) Crack pattern

Fig. 10 Result of FEA of Iwata brick chimney

σ'_i is reduced in the region of tension-compression as follows.

$$\sigma'_i = f'_i(1 + \sigma_2/f'_c) \quad (6)$$

where σ'_i denotes the cracking stress. σ_2 and f'_i are the compressive stress perpendicular to the tensile stress and the uni-axial tensile strength, respectively.

Structural characteristics of the brick chimneys are considered through material and geometrical non-linear analyses. Material constants used in the analysis are Young's modulus $E = 3200$ MPa, Poisson's ratio $\nu = 0.15$, weight per unit volume $\gamma = 16.5$ kN/m³, ultimate tensile strength $f'_t = 0.37$ MPa derived by static collapse test, ultimate compressive strength $f'_c = 7.5$ MPa, ultimate compressive strain $\varepsilon_c = 0.003$, tension stiffening parameters $\varepsilon_m = 0.002$ and $\alpha = 0.5$ (Fig. 8).

7.2 Results of static non-linear analysis

Fig. 9 shows deformation and crack pattern of Howa brick chimney. From the results of FEA (Finite Element Analysis), as shown in Fig. 9(b), collapse occurs at the middle height of the chimney. This collapse mechanism corresponds well to that of experimental result (Photo 3(b)). On the other hand, deformation and crack pattern of Iwata brick chimney are shown in Fig. 10. Collapse occurs at the base of the chimney which corresponds well to that of experimental result (Photo 4(b)).

Fig. 11 shows relationship between horizontal load and displacement of Howa and Iwata brick chimneys obtained by FEA comparing with those of experimental results. From these Figures, ultimate horizontal loads obtained by FEA correspond well to their ultimate experimental horizontal ones.

Fundamental frequencies determined by eigenvalue analysis are listed in Table 3 comparing with the results identified by ARMAV model.

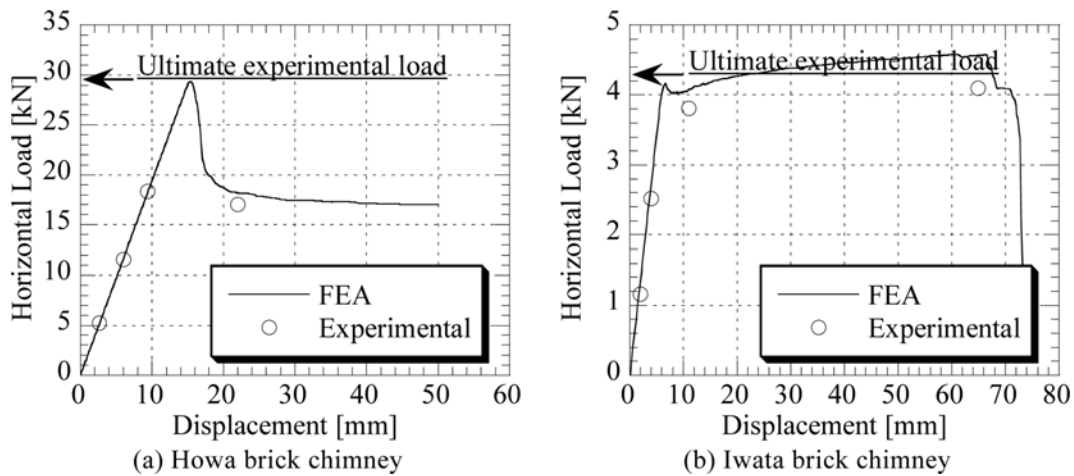


Fig. 11 Relationship between horizontal load and displacement

Table 3 Fundamental frequencies determined by FEA comparing with the results of ARMAV

	Direction	Mode	Natural frequency (Hz)	
			ARMAV	FEA
Howa	North-South	1st	3.0603	2.7572
		2nd	9.9725	11.1547
		3rd	22.3372	25.6448
	East-West	1st	2.6918	2.6924
		2nd	9.3494	10.9514
		3rd	22.7584	25.4511
Iwata	North-South	1st	2.9330	2.9547
		2nd	14.4932	15.5084
		3rd	21.8729	23.0881
	East-West	1st	2.9356	2.9547
		2nd	13.7789	15.5084
		3rd	19.9204	23.0881

8. Seismic performance of brick chimneys

The numerical models, updated on the basis of the results of static and dynamic tests, are used in this section to estimate the seismic response of the two brick chimneys. In the European code, that is Eurocode n.8: “Design of structures for earthquake resistance”, non-linear static (Pushover) analysis is available for this purpose.

8.1 Pushover analysis

Pushover analysis is a non-linear static analysis under constant gravity loads and monotonically

increasing horizontal loads. It may be applied to verify the structural performance of newly designed and of existing structures.

Pushover analysis needs the following steps:

- 1) Evaluation of the relation between base shear force F_b and the control displacement d_c (the “capacity curve”)

The capacity curve should be determined by pushover analysis. As for the lateral loads, at least two vertically distributed lateral loads should be applied.

- a) an “uniform” pattern, based on lateral forces that are proportional to mass given by

$$F_i = \frac{m_i}{\sum_{j=1}^n m_j} F_b \tag{7}$$

where F_b is base shear force of the MDOF (multi degrees of freedom) system, n is the number of stories, m_i is the mass in the i -th story.

- b) a “modal” pattern, proportional to 1st mode shape given by

$$F_i = \frac{m_i \cdot \Phi_{1i}}{\sum_{j=1}^n (m_j \cdot \Phi_{1j})} F_b \tag{8}$$

where Φ_1 is normalized displacement of 1st mode shape.

- 2) Transformation to an equivalent SDOF system

In the elastic phase, the force F^* and the displacement d^* of the equivalent single degree of freedom (SDOF) system are computed as (Fig. 12):

$$F^* = F_b/\Gamma, \quad d^* = d_c/\Gamma \tag{9}$$

where Γ is the transformation factor $\Gamma = \frac{\sum m_i \Phi_i}{\sum m_i \Phi_i^2}$, d_c is control nodal displacement of MDOF system.

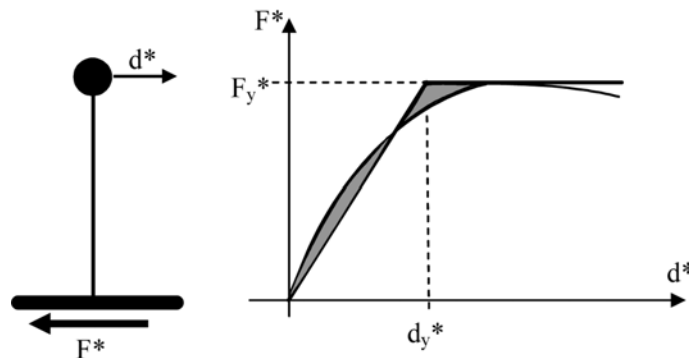


Fig. 12 Equivalent of SDOF system. Relationship between the idealized elasto-perfectly plastic force and displacement

The yield force F_y^* , which represents also the ultimate strength of the idealized system, and the yield displacement of the idealized SDOF system d_y^* are given by (Fig. 12):

$$F_y^* = F_{bu}/\Gamma, \quad d_y^* = F_y^*/k^* \tag{10}$$

where F_{bu} is the ultimate strength of the structure, k^* is the initial stiffness of the idealized system.

3) Determination of the period of the idealized equivalent SDOF system

By using the mass of an equivalent SDOF system m^* , the period of the idealized equivalent SDOF system is determined by:

$$T^* = 2\pi \sqrt{\frac{m^*}{k^*}}, \quad m^* = \sum_{i=1}^n m_i \Phi_{i,1} \tag{11}$$

4) Determination of the target displacement for the equivalent SDOF system

As shown in Fig. 13, the target displacement of the structure with period T^* and unlimited elastic behaviour is given by:

$$\begin{aligned} \text{if } T^* > T_C & \quad d_{\max}^* = d_{e, \max} = S_{De}(T^*) \\ \text{if } T^* < T_C & \quad d_{\max}^* = \frac{d_{e, \max}}{q^*} \left[1 + (q^* - 1) \frac{T_C}{T^*} \right] \geq d_{e, \max} \end{aligned} \tag{12}$$

Where T_C is corner period at the upper limit of the constant acceleration region of the elastic Spectrum, $S_{De}(T^*)$ is the elastic acceleration response spectrum at the period T^* and q^* is the ratio

between the accelerations in the structure with unlimited elastic behavior $q^* = \frac{S_e(T^*)m^*}{F_y^*}$.

5) Determination of the target displacement for the MDOF system

The target displacement of the MDOF system, corresponding to the control node, is given by:

$$d_i = d^* \cdot \Gamma \tag{13}$$

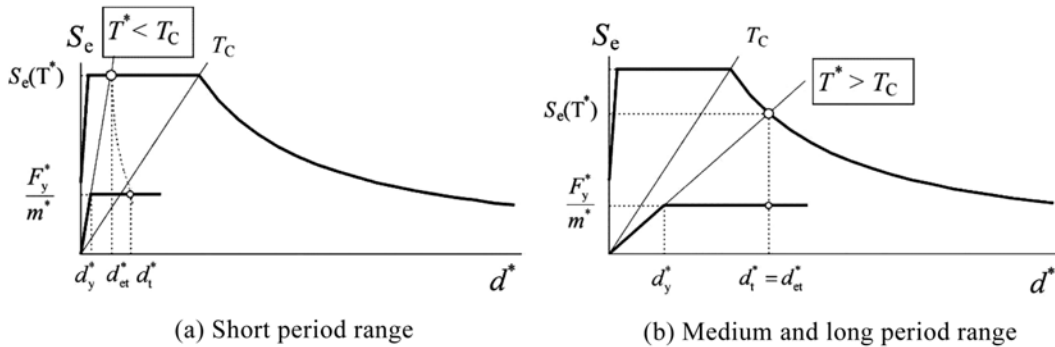


Fig. 13 Determination of the target displacement for the equivalent SDOF system

8.2 Result of static non-linear (Pushover) analysis

Non-linear (Pushover) analysis is executed to Howa and Iwata brick chimneys applying a “modal” pattern type of horizontal forces (proportional to 1st mode shape) linearly increasing until their collapse. As a result of non-linear response, relationships between horizontal load and displacement of Howa and Iwata brick chimneys are shown in Fig. 14, respectively. In Fig. 14, dotted line represents the relationship between the force F^* and the displacement d^* of the equivalent SDOF system. Ultimate displacements at the top of Howa and Iwata brick chimneys are about 127 mm and 72 mm, respectively. Solid bold line represents the response of the equivalent bi-linear SDOF

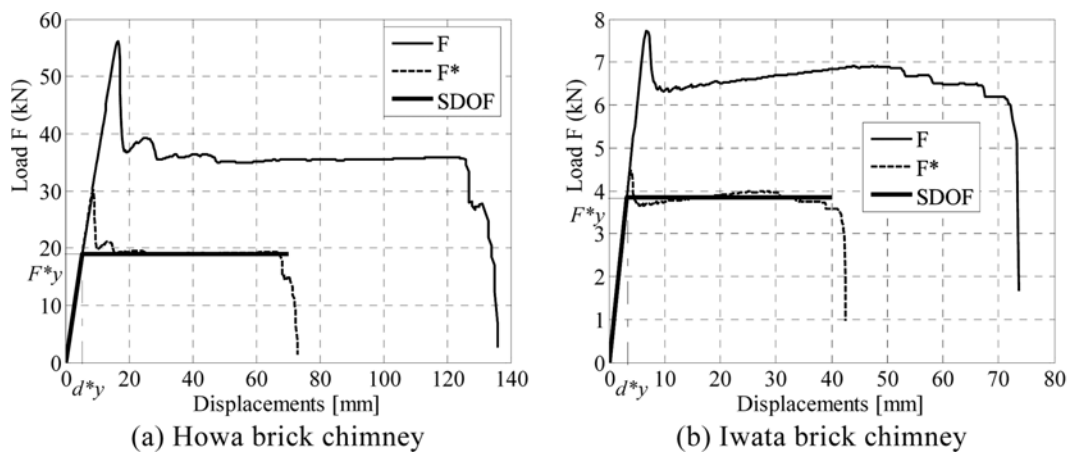


Fig. 14 Relationship between horizontal load and displacement determined by Pushover analysis

Table 4 Properties of equivalent SDOF system

	Γ	F^*y (N)	k^* (N/m)	d^*y (m)	T^* (s)
Howa	1.862	19000	3502800	0.0054	0.346
Iwata	1.732	3850	1192700	0.0032	0.286

Table 5 Target displacements of MDOF system (mm)

a/g	Howa brick chimney					Iwata brick chimney				
	Ground type					Ground type				
	A	B	C	D	E	A	B	C	D	E
0.15	24	33	35	52	39	16	24	26	40	28
0.25	40	58	64	96	68	29	42	47	73	50
0.35	57	83	92	139	97	41	60	68	106	71
0.50	82	120	135	205	141	59	88	100	156	104
0.70	115	170	193	293	199	84	125	142	223	147
0.85	140	208	236	359	243	102	153	174	272	179
1.00	165	245	279	424	287	121	180	206	322	211

Table 6 Ground types

Ground type	Description
A	Rock or other rock-like geological formation, including at most 5 m of weaker material at the surface
B	Deposits of very dense sand, gravel, or very stiff clay, at least several tens of m in thickness, characterised by a gradual increase of mechanical properties with depth
C	Deep deposits of dense or medium-dense sand, gravel or stiff clay with thickness from several tens to many hundreds of m
D	Deposits of loose-to-medium cohesionless soil (with or without some soft cohesive layers), or of predominantly soft-to-firm cohesive soil
E	A soil profile consisting of a surface alluvium layer with v_s values of type C or D and thickness varying between about 5 m and 20 m

system in Fig. 14. The characteristics of the equivalent bi-linear SDOF systems are summarized in Table 4.

The target displacements evaluated from Eqs. (12) and (13) considering the ground type (Table 6) and the design ground acceleration a are listed in Table 5. From Table 5, the target displacement of Howa brick chimney is 139 mm if the value of a/g equals 0.35 and the ground type is *D*. It is larger than the limit value of 127 mm determined by pushover analysis (Fig. 14(a)). On the other hand, under the same condition as Howa brick chimney, the target displacement of Iwata brick chimney is 73 mm and it is larger than the limit value of 72 mm determined by pushover analysis (Fig. 14(b)). According to the static non-linear (Pushover) analysis, Howa and Iwata brick chimneys seem to be vulnerable to earthquakes with 0.35 and 0.25 g, respectively.

9. Conclusions

The following concluding remarks were obtained:

- 1) From the material tests, Young's modulus and compressive strength of the brick used for these chimneys are estimated to be 3200 MPa and 7.5 MPa, respectively.
- 2) The results of static collapse test of the existing two brick chimneys are discussed comparing with the results obtained by FEA. Ultimate horizontal loads obtained by FEA correspond well to their ultimate experimental horizontal ones.
- 3) From the results of dynamic tests, the fundamental frequencies of Howa and Iwata brick chimneys are estimated to be about 2.79 Hz and 2.93 Hz, respectively. Their natural modes are identified by ARMAV model.
- 4) According to the static non-linear (Pushover) analysis, these brick chimneys seem to be vulnerable to earthquakes with 0.25 to 0.35 g.

Acknowledgements

The authors wish to appreciate the cooperation of Mr. Tomizou Kakita of Ex-director of INAX

Kiln Plaza and Museum, Mr. Keizo Umehara of Tokoname City, and Mrs. Keiko Sughie of the representative of Tokoname hometown circle "Tsuchinoko". The financial supports were offered by Grants-in-Aid for Scientific Research (Kakenhi), The Hibi Research Grant, Tokai Academic Encouragement Grant and The Grant-in-Aid for Research in Nagoya City University.

References

- Ahmad, S., Irons, B.M. and Zienkiewicz, O.C. (1970), "Analysis of thick and thin shell structures by curved finite elements", *Int. J. Numer. Meth. Eng.*, **2**, 419-451.
- Andersen, P., Brincker, R. and Kirkegaard, P.H. (1996), "Theory of covariance equivalent Arnav models of civil engineering structures", *Proc. of the 14th Int. Modal Analysis Conf. (IMAC)*, Dearborn, Michigan, 518-524.
- Andersen, P. and Kirkegaard, P.H. (1998), "Statistical damage detection of civil engineering structural using Arnav models", *Proc. of the 16th Int. Modal Analysis Conf. (IMAC)*, Santa Barbara, California, 356-362.
- Anthoine, A. (1995), "Numerical simulations of tests performed on a masonry building prototype", *Experimental and Numerical Investigation on a Brick Masonry Building Prototype - Numerical Prediction of the Experiment*, Report 3.0, G.N.D.T., Pavia.
- Aoki, T., Kato, S., Ishikawa, K., Hidaka, K., Yorulmaz, M. and Çili, F. (1997), "Principle of structural restoration for Hagia Sophia dome", *Structural Studies, Repairs and Maintenance of Historical Buildings V*, 467-476.
- Aoki, T. (2001), "Formulation of elastic-plastic joint elements and their application to practical structures", *Computational Modelling of Masonry, Brickwork and Blockwork Structures*, ed. by Bull, J.W., Saxe-Coburg Publications, 27-52.
- Aoki, T., Carpentieri, D., De Stefano, A., Genovese, C. and Sabia, D. (2001), "Analisi sismica di parete in muratura: Metodi e tecniche a confronto", *Proc. of X convegno nazionale ANIDIS on l'ingegneria sismica in Italia*, Potenza, 1-12 (CD-ROM) (in Italian).
- Aoki, T. and Sato, T. (2003a), "Application of Bott-Duffin inverse to static and dynamic analysis of masonry structures", *Structural Studies, Repairs and Maintenance of Heritage Architecture VIII*, WIT Press/Computational Mechanics, 277-286.
- Aoki, T. and Sabia, D. (2003b), "Collapse analysis of masonry arch bridges", *Proc. of the Ninth Int. Conf. on Civil and Struct. Eng. Comp.*, Egmond aan Zee, The Netherlands, September, 1-14 (CD-ROM).
- Aoki, T. (2004), "Brick chimneys in Tokoname", *Invitation to Design and Architecture VIII*, Gifu Newspaper Inc., 166-198 (in Japanese).
- Aoki, T. and Sabia, D. (2004), "Theoretical and experimental analysis of brick chimneys, Tokoname, Japan", *Computational Mechanics, Proc. of WCCM VI in Conjunction with APCOM'04*, Beijing, September, 1-12 (CD-ROM).
- De Stefano, A., Sabia, D. and Sabia, L. (1997), "Structural identification using ARMAV models from noisy dynamic response under unknown random excitation", *Proc. of DAMAS Int. Conf.*, Sheffield, 419-428.
- De Stefano, A., Ceravolo, R. and Sabia, D. (2001), "Output only dynamic identification in time-frequency domain", *Proc. of 2001 American Control Conf.*, Arlington.
- Eurocode n.8 (2003), "Design of structures for earthquake resistance", European standard prEN 1998-1, Doc CEN/TC250/SC8/N335.
- Gambarotta, L. and Lagomarsino, S. (1997a), "Damage models for the seismic response of brick masonry shear walls. Part I: The mortar joint model and its applications", *Earthq. Eng. Struct. Dyn.*, **26**, 423-439.
- Gambarotta, L. and Lagomarsino, S. (1997b), "Damage models for the seismic response of brick masonry shear walls. Part II: The continuum model and its applications", *Earthq. Eng. Struct. Dyn.*, **26**, 441-462.
- Garibaldi, L., Giorcelli, E., Marchesiello, S. and Ruzzene, M. (1999), "CVA-BR against ARMAV: comparison over real data from an ambient noise excited bridge", *Key Engineering Materials*, **167-168**, 423-431.
- Garibaldi, L., Marchesiello, S., Giorcelli, E. and Gorman, D.J. (2001), "CVA and ARMAV: performance comparison over real data", *J. Intelligent Material Systems and Structures*, **12**(8), 577-588.
- Giorcelli, E., Garibaldi, L. and Piombo, B. (1998), "ARMAV techniques for traffic excited bridges", *ASME J. Vibration and Acoustics*, July, 713-718.

- Hinton, E. and Owen, J. (1984), *Finite Element Software for Plates and Shells*, Pineridge Press.
- Hughes, T.J.R. and Cohen, M. (1978), "The 'Heterosis' finite element for plate bending", *Comput. Struct.*, **9**, 445-450.
- Hughes, T.J.R. and Hinton, E. (1986), *Finite Element Methods for Plates and Shell Structures - Vol. 1 Element Technology*, Pineridge Press.
- Kato, S., Hidaka, K. and Aoki, T. (1986), "A study on the formulation of a elastic-plastic joint element by truss elements - An application of the theory of effective strength", *Trans. of A.I.J.*, **370**, 50-59 (in Japanese).
- Kupfer, H., Hilsdorf, K.H. and Rush, H. (1969), "Behavior of concrete under biaxial stresses", *ACI J.*, **66**(8), 656-666.
- Kupfer, H. and Gerstle, K.H. (1973), "Behavior of concrete under biaxial stresses", *J. of the Eng. Mech. Div.*, ASCE, **99**(EM4), 853-866.
- Lourenço, P.B., Rots, J.G. and Blaauwendraad, J. (1995), "Two approaches for the analysis of masonry structures: Micro and macro-modeling", *HERON*, **40**(4), 313-340.
- Magenes, G., Calvi, G.M. and Kingsley, R. (1995), "Seismic testing of a full-scale, two-story masonry building: test procedure and measured experimental response", *Experimental and Numerical Investigation on a Brick Masonry Building Prototype - Numerical Prediction of the Experiment*, Report 3.0, G.N.D.T., Pavia.
- Magenes, G. and Calvi, G.M. (1997), "In-plane seismic response of brick masonry walls", *Earthq. Eng. Struct. Dyn.*, **26**, 1091-1112.
- Marple, L. Jr. (1987), *Digital Spectral Analysis with Applications*, Prentice Hall, Englewood Cliffs.
- Olafsson, S. and Sigbjörnsson, R. (1995), "Application of ARMA models to estimate earthquake ground motion and structural response", *Earthq. Eng. Struct. Dyn.*, **24**, 951-966.
- Page, A.W. (1981), "The biaxial compressive strength of brick masonry", *Proc. Intsn. Civ. Engrs.*, Part 2, **71**, 893-906.
- Page, A.W. (1983), "The strength of brick masonry under biaxial compression-tension", *Int. J. Masonry Constr.*, **3**(1), 26-31.
- Peeters, B. and De Roeck, G. (2001), "Stochastic system identification for operational modal analysis: A review", *J. Dynamic Systems, Measurement, and Control*, **123**, 1-9.
- Sabia, D., Bonisoli, E., Fasana, A., Garibaldi, L. and Marchesiello, S. (2003), "Advances in identification and fault detection in bridge structures", *Key Engineering Materials*, **245-246**, 339-350.
- Tokoname City web site, http://www.city.tokoname.aichi.jp/html/intro_e/top.html
- Zienkiewicz, O.C. (1971), *The Finite Element in Engineering*, McGraw-Hill.